Impact of Substrate Corrugation on the Sliding Friction Levels of Adsorbed Films

T. Coffey* and J. Krim

Physics Department, Box 8202, North Carolina State University, Raleigh, North Carolina 27695-8202, USA

(Received 13 May 2005; published 10 August 2005)

We report a quartz crystal microbalance (QCM) study of sliding friction for solid xenon monolayers at 77 K on Cu(111), Ni(111), graphene/Ni(111), and C_{60} substrates. Simulations have predicted a strong dependence of phononic friction coefficient (η) on surface corrugation in systems with similar lattice spacing, $\eta \propto U_0^2$, but this has never before been shown experimentally. In order to make direct comparisons with theory, substrates with similar lattice spacing but varying amplitudes of surface corrugation were studied. QCM data reveal friction levels proportional to U_0^2, validating current theoretical and numerical predictions. Measurements of Xe/C_{60} are also included for comparison purposes.

DOI: 10.1103/PhysRevLett.95.076101 PACS numbers: 68.35.Af, 68.43.Pq, 68.60.−p

The ability to predict sliding friction in an adsorbed film system is key to a vast range of fundamental and applied issues in physics and nanotechnology. Whether attempting to unravel basic mysteries associated with the existence of static friction [1] or ''simply'' seeking to design an atomic-scale automobile [2], such knowledge is paramount. Progress in this important topic has, however, been extremely slow, as theoretical predictions of sliding friction have heretofore involved experimentally inaccessible systems.

Sliding friction levels in adsorbed monolayers can be measured experimentally by means of the quartz crystal microbalance (QCM) technique [3,4] and are also amenable to theoretical treatments, including both analytic calculations and molecular-dynamics simulations [5–9]. A value for the ''binding potential'' that holds the monolayer to the substrate is, however, required in order to compare the experimental measurements to theory. While the average value for the binding potential can be determined by a variety of methods, the ''corrugation potential,'' or variation of the binding potential horizontally along the surface, is known for only an extremely limited number of experimental systems. Numerical simulations have predicted a strong dependence of the phononic friction coefficient, η_p, on surface corrugation, U_0, in systems with similar lattice spacing, $\eta_p \propto U_0^2$ [5]. To date, this has been extremely difficult to show experimentally, as systems with different surface corrugations generally have dissimilar lattice spacing. We report here the first measurements of sliding friction in systems with independently determined corrugation potentials, allowing for the first time a direct comparison of theory and experiment in an environment free of adjustable parameters.

The first measurements of sliding friction in adsorbed monolayers were reported in 1991 and 1996, for the systems Kr/Au(111) [10] and Xe/Ag(111) [11], respectively. The experiments generated much theoretical interest, and a variety of approaches were employed in order to understand the fundamental energy dissipation processes that gave rise to the reported friction levels. All of the models employed a sinusoidal interaction potential for the noble gas atoms with the metal substrate. Such potentials are corrugated with U_0 generally defined as the amplitude of the periodic function describing the changes in adsorbate-substrate potential with respect to adsorbate position. One of the surprising results revealed by the experiments was the fact that both solid and liquid monolayers of the adsorbed films were well described by the (static-friction free) ''viscous friction'' law $F = -(m/\tau)v = -m\eta v$. In this relation F is friction force, m is mass of the adsorbed film, and v is average film sliding speed. The slip time τ, which is inversely proportional to the friction level, is a characteristic time for friction to decrease to $1/e$ of the original sliding speed v. The viscous coefficient of friction, η, is frequently parametrized in the following manner [8]:

$$\eta = \eta_{\text{subs}} + aU_0^2. \tag{1}$$

Here η_{subs} is the damping, or dissipation, of the adsorbate sliding energy within the substrate (from both phononic and electronic friction), and a is a constant depending on temperature and lattice spacing. The aU_0^2 term arises from phononic energy dissipation in the adlayer.

Phononic friction arises from sliding-induced atomic vibrations, or sound waves. The energy expended in exciting these vibrations is ultimately transformed into heat. Electronic mechanisms for friction in electrically conducting materials are due to sliding-induced excitation of conduction electrons at metallic interfaces. All of the modeling efforts cited above successfully fit the data from the QCM friction results, but with substantially varying ratios of electronic to phononic friction.

It is difficult to determine which group employed the most realistic theoretical model because independent experimental or theoretical values for the corrugation potential in the systems Kr/Au(111) and Xe/Ag(111) have not been reported. Indeed, U_0 has been measured for only a very few systems. These include helium atom scattering (HAS) and related spectroscopy [12,13] measurements of U_0 for the systems Xe/Cu(111) and Xe/graphite and surface diffusion measurements of U_0 for Xe/Ni(111). (Table I [13–17].) Since Cu(111) and Ni(111) have very

TABLE I. The surface corrugations, substrate spacing, overlayer spacing, and monolayer slip times for Ag(111) [11,14], Cu(111) [13], Ni(111) [15], graphene/Ni(111) [16], and C_{60} [17]. The Xe/C_{60} spacing is deduced from the frequency shift at 1.2 mTorr. The slip time uncertainties are 45%.

System	U_0 (meV)	Substrate Spacing (nm)	Xenon Spacing (nm; atoms/nm^2)	Slip time (ns)
Ag(111)	0.69–2.7	0.288	0.439–0.452; 5.65–5.99	2.0
Cu(111)	1.9	0.255	0.4414; 5.93	15.5
Ni(111)	14	0.249	0.441; 5.94	0.47
Graphene/Ni(111)	5.3	0.249	0.441; 5.94	1.7
C_{60}/Ag(111)	Large??	1.00	0.45; 5.7	5.5

similar lattice spacings, they are ideal for testing Eq. (1), since numerical simulations of Eq. (1) have used a single lattice spacing [5,8]. Graphene (a graphitic layer one atom thick) can additionally be grown epitaxially on top of a Ni(111) substrate so as to have the same lattice spacing as Ni(111), rather than that of natural graphite [18].

QCM friction measurements are performed by adsorbing xenon under equilibrium conditions onto the surface electrodes of the oscillator. Film adsorption onto the microbalance produces shifts in both the frequency and amplitude of vibration, which are simultaneously recorded as a function of pressure. Changes in resonant frequency of the microbalance, δf, are proportional to the fraction of the mass of the condensed film that is able to track the oscillatory motion of the underlying substrate [19]. Amplitude shifts are due to frictional shear forces exerted on the surface electrode by the adsorbed film. Characteristic slip times, τ, are determined via $\delta(Q^{-1}) = 4\pi\tau(\delta f)$ [3,4]. [Amplitude shifts are converted to quality factor shifts $\delta(Q^{-1})$ through helium gas calibration or via a ''ring-down'' method [3].]

The relation between the frequency shift of a film if it were not slipping (δf_{film}) and the experimentally observed frequency shift (δf) is as follows: [20]

$$\frac{\delta f_{\text{film}}}{f} = -\frac{2m_f c_f}{\rho_q t_q} \qquad \delta f = \frac{\delta f_{\text{film}}}{1 + (\omega\tau)^2}. \tag{2}$$

Here, $m_f c_f$ are the atomic mass in grams and coverage in atoms per cm^2 of the adsorbed film, and ρ_q (2.65 g/cm^3) and t_q (0.021 cm for $f = 8$ MHz) are the density and thickness of the QCM. While technically some of the mass of the film will be always be decoupled from the oscillation, the frequency shift will be only be substantially reduced for systems characterized by slip times nearing or exceeding the condition $2\pi f\tau = 1$. Changes in frequency and quality factor due to gas pressure, tensile stress, and temperature effects were negligible in this experiment.

The QCMs used in this work consisted of a single crystal of overtone-polished AT-cut quartz that oscillated in transverse shear motion with a quality factor Q near 10^5. The driving force, supplied here by a Pierce oscillator circuit, has constant magnitude and is periodic with frequency $f =$ 8 MHz, the series resonant frequency of the oscillator.

For the Cu(111) sample, the copper was deposited atop a QCM with a 20 nm titanium precoat to produce an extremely flat copper electrode [21]. The base pressure of the vacuum system ranged from 8×10^{-11} to 5×10^{-10} Torr. Thermal evaporation was then used to deposit 60 nm of 99.999% pure Cu atop the titanium precoat or blank QCM, respectively, producing a mosaic structure with a (111) fiber texture [22]. C_{60} substrates were prepared by thermally evaporating 2 monolayers of C_{60} atop an 80 nm thick Ag(111) electrode on a blank QCM. Like the Cu(111), the Ag(111) was prepared via thermal evaporation of 99.999% pure Ag, and the C_{60} was deposited immediately after the Ag(111) deposition. The 80 nm Ni(111) films were deposited using an electron beam evaporator in ultrahigh vacuum (UHV) onto a blank QCM. The deposition rate was several angstroms per second. The graphene samples were prepared by heating the Ni(111) samples to 500 °C while dosing the sample with 10^{-6} Torr of carbon monoxide. The nickel then acts as a catalyst, forming a pure graphitic carbon onto the nickel surface and sending biproducts of carbon dioxide and nickel carbide into the gas phase [18].

After preparation, all samples were immediately transferred *in situ* to the adsorption cell where they were electrically connected to an external Pierce oscillator circuit. They were then chilled to 77.4 K by submersion in a liquid nitrogen bath. After the samples had come to thermal equilibrium, they were exposed to research grade xenon gas while frequency and amplitude shifts were monitored as a function of pressure.

The raw frequency shift and quality factor data for the xenon uptake on Cu(111), Ni(111), and graphene/Ni(111) are shown in Fig. 1. The stepwise nature of the data is characteristic of layer by layer formation of atomic monolayers and indicates that the substrate films are clean and have atomically flat regions (30 nm)^2 or more in size [23]. Note that the frequency shift data for the Cu(111) sample underrepresent the actual mass of the adsorbed film on account of film slippage effects [Eq. (2)].

The slip times for xenon on Cu(111), Ni(111), and graphene/Ni(111) versus coverage c_f, as determined from Eq. (2), (i.e., corrected for slippage) are shown in Fig. 2. From highest to lowest xenon slip time, the surfaces are Cu(111), graphene, and Ni(111). The Xe/C_{60} isotherm and Xe/C_{60} slip time are shown separately in Figs. 3(a) and 3(b). The ''compressed monolayer'' slip times (corresponding to roughly 6 atoms per nm^2) are shown in Table I.

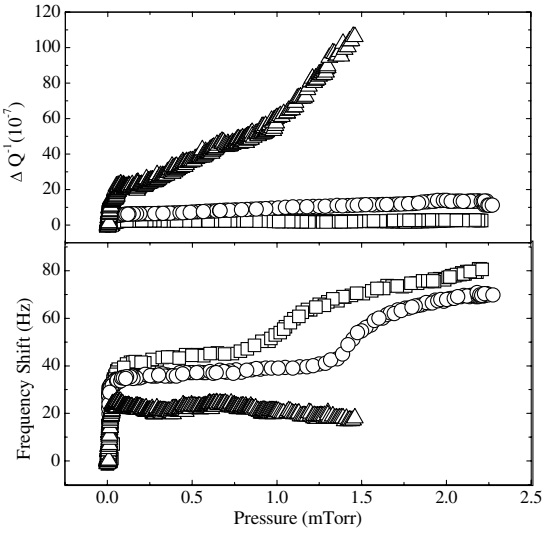

FIG. 1. Xenon mass uptake and quality factor shift (raw data) for Cu(111) (triangles), Ni(111) (squares), and graphene/Ni(111) (circles).

Figure 4 displays the natural log of the xenon monolayer slip time τ in seconds versus the natural log of the adsorbate/substrate corrugation U_0 in meV. Setting $\eta = m/\tau$ in Eq. (1) (m is adsorbate mass) and solving for τ, one obtains $\tau = 1/(\eta_{\text{subs}} + aU_0^2)$. Upon taking the natural log, one obtains $\ln(\tau) = -\ln(\eta_{\text{subs}} + aU_0^2)$. Under the assumption that $\eta_{\text{subs}} < aU_0^2$ [24], this can be expanded as follows:

$$\ln(\tau) = \left[-\ln(a) - 2\ln(U_0) - \frac{\eta_{\text{subs}}}{aU_0^2} + \cdots \right]. \quad (3)$$

Therefore, when plotting $\ln(\tau)$ versus $\ln(U_0)$, the above equation suggests the data should be well fit with a slope of -2 if the expansion terms are neglected. The data for systems with similar lattice spacing (Xe/Cu(111), Xe/Ni(111), and Xe/graphene) are fit with a slope of -1.8 ± 0.2 and an intercept of 3.8 ± 0.4; see Fig. 4.

If we assume that τ obeys $\tau = 1/(\eta_{\text{subs}} + aU_0^2)$, then we can use a nonlinear fit on our slip time data and solve for the constants η_{subs} and a. At "compressed monolayer" coverage, the best fit yields a negligibly small value for η_{subs}, 1×10^{-15} ns^{-1} and $a = 0.018 \pm 0.01$ ns^{-1} meV^{-2}. At coverage of 0.94 monolayers (approximately 5.6 atoms/nm^2), the fit yields $\eta_{\text{subs}} = 1 \times 10^{-16}$ ns^{-1} (also negligible) and $a = 0.020 \pm 0.01$ ns^{-1} meV^{-2}. Liebsch *et al.* [8] found $a = 0.028$ ns^{-1} meV^{-2} at a coverage of 0.94 monolayers. (We note that we define the total barrier height as U_0, while Liebsch *et al.* defined the "corrugation" as $U_0/4.5$.) Regarding the uncertainty in η_{subs}, the uncertainty in the experimental slip times allows for an upper bound on η_{subs} of 0.08 ns^{-1}.

The monolayer slip times of Xe/Ag(111) [11] and Xe/C_{60} are also plotted in Fig. 4 using estimated values of U_0. It is reasonable to assume that the dissimilar conditions in

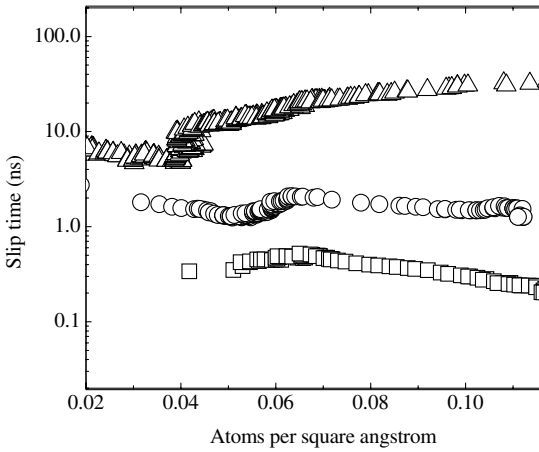

FIG. 2. The slip times for xenon on Cu(111) (triangles), Ni(111) (squares), and graphene/Ni(111) (circles) vs coverage. The coverage (corrected for slip effects) is obtained by solving the right expression in Eq. (2) for (δf_{film}) and then substituting the value into the left expression in Eq. (2). The frequency shift of a monolayer of xenon is calculated from the xenon mass and spacings (coverage) given in Table I. Compressed monolayer coverage is 6 atoms/nm^2, corresponding to 1.31×10^{-12} ng/nm^2.

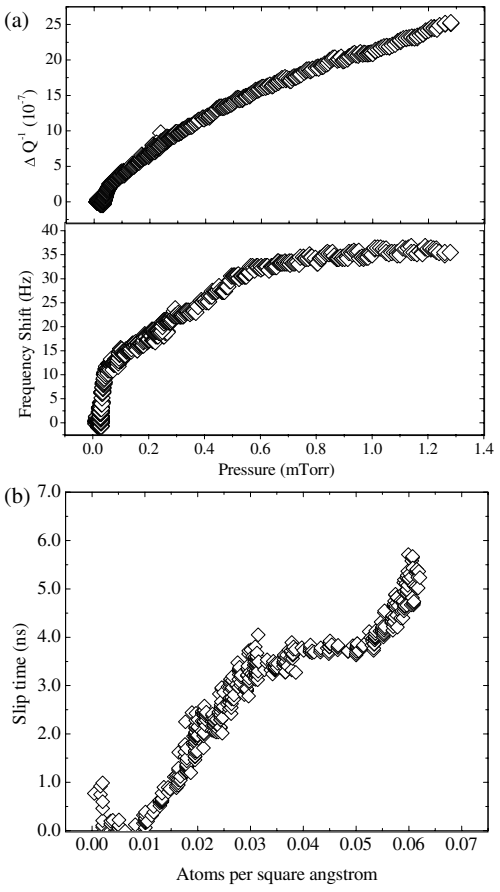

FIG. 3. (a) Xenon mass uptake and quality factor shift (raw data) for C_{60}/Ag(111). (b) Slip time for xenon sliding on C_{60}/Ag(111). Note that the slip time is zero for coverages less than 0.01 atoms/angstrom^2.

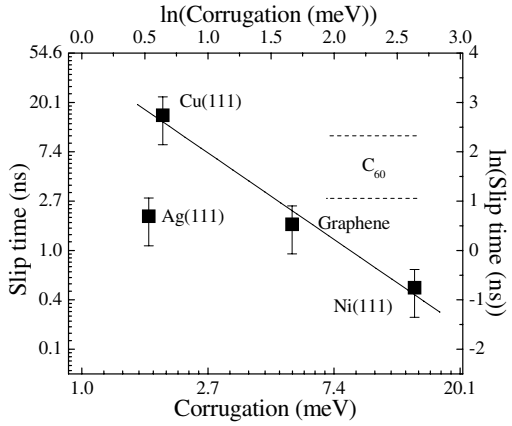

FIG. 4. Slip time vs surface corrugation. The corrugation value for Xe/Ag(111) is estimated here as 1.7 meV. The dashed lines around the C_{60} represent the uncertainty in slip time. The corrugation of Xe/C_{60} is unknown.

lattice spacing for the Xe/Ag(111) and Xe/C_{60} experiments cause the deviation from the fitted slope of -2.

It should be noted that Xe/Cu(111) at 77 K is a commensurate system [13], and that Xe/Ni(111) and Xe/graphene are not commensurate systems [15]. Many other experiments [25] show that commensurate systems have very high sliding friction, or even that the films ''lock down'' onto the substrate. In our results, however, the commensurate Xe/Cu(111) system has the highest slip time, or lowest friction. It has been observed numerically [5] that systems with low surface corrugation will slip, even in commensurate systems. The Xe/Cu(111) system has the lowest surface corrugation of the systems studied, and this may explain the high slippage of the xenon film. In contrast, in the Xe/C_{60} system, which should have high surface corrugation, the xenon film does lock down (no slipping) for certain coverages. This may indicate a commensurate phase at low coverage, where the xenon atoms lie in the valleys of the C_{60} surface potential.

In conclusion, we have shown the first direct experimental evidence that the friction coefficient is proportional to the square of the surface corrugation for systems with similar lattice spacing, validating current theoretical predictions. We have also provided evidence that the friction studied herein is primarily of phononic origin. Many past experimental studies have performed friction measurements, but little direct evidence of the source of the friction has been given. We have also shown the importance of lattice spacing in predictions of phononic friction, as systems with dissimilar spacing deviate from the $\eta \propto U_0^2$ fits. Finally, we have performed friction measurements on the Xe/C_{60} system, which should be readily modeled by means of numerical simulation.

This work has been supported in part by the NSF Grant No. DMR0320743, DOE Grant No. FG02-01ER45936, and AFOSR Grant No. F49620014-0132. S. M. Winder is thanked for useful discussions, technical assistance, and data collection.

*Currently at Department of Physics and Astronomy, Appalachian State University, CAP Bldg., 525 Rivers St., Boone, NC 28608.

[1] M. H. Muser, L. Wenning, and M. O. Robbins, Phys. Rev. Lett. **86**, 1295 (2001); G. He, M. H. Muser, and M. O. Robbins, Science **284**, 1650 (1999).
[2] M. Porto, M. Urbakh, and J. Klafter, Phys. Rev. Lett. **84**, 6058 (2000).
[3] E. T. Watts, J. Krim, and A. Widom, Phys. Rev. B **41**, 3466 (1990); M. Rodahl *et al.*, Rev. Sci. Instrum. **66**, 3924 (1995).
[4] J. Krim and A. Widom, Phys. Rev. B **38**, 12184 (1988); L. Bruschi and G. Mistura, Phys. Rev. B **63**, 235411 (2001).
[5] M. Cieplak, E. D. Smith, and M. O. Robbins, Science **265**, 1209 (1994).
[6] B. N. J. Persson and A. Nitzan, Surf. Sci. **367**, 261 (1996).
[7] M. S. Tomassone, J. B. Sokoloff, A. Widom, and J. Krim, Phys. Rev. Lett. **79**, 4798 (1997).
[8] A. Liebsch, S. Goncalves, and M. Kiwi, Phys. Rev. B **60**, 5034 (1999).
[9] M. O. Robbins and M. H. Muser, in *CRC Handbook of Modern Tribology*, edited by B. Bhushan (CRC Press, Boca Raton, FL, 2000).
[10] J. Krim, D. H. Solina, and R. Chiarello, Phys. Rev. Lett. **66**, 181 (1991).
[11] C. Daly and J. Krim, Phys. Rev. Lett. **76**, 803 (1996).
[12] L. W. Bruch, Phys. Rev. B **37**, 6658 (1988).
[13] J. Braun, D. Fuhrmann, A. Siber, B. Gumhalter, and Ch. Woll, Phys. Rev. Lett. **80**, 125 (1998); M. A. Chesters, M. Hussain, and J. Pritchard, Surf. Sci. **35**, 161 (1973).
[14] L. W. Bruch (private conversation).
[15] E. Nabighian and X. D. Zhu, Chem. Phys. Lett. **316**, 177 (2000); D. Fargues, P. Dolle, M. Alnot, and J. J. Ehrhardt, Surf. Sci. **214**, 187 (1989).
[16] R. Kariotis, J. A. Venables, M. Hamichi, and A. Q. D. Faisal, J. Phys. C **20**, 5717 (1987).
[17] T. Sakurai, X. D. Wang, T. Hashizume, V. Yurov, H. Shinohara, and H. W. Pickering, Appl. Surf. Sci. **87/88**, 405 (1995).
[18] J. Nakamura, H. Hirano, M. Xie, I. Matsuo, T. Yamada, and K. Tanaka, Surf. Sci. **222**, L809 (1989).
[19] G. Z. Sauerbrey, Phys. Verhandl. **8**, 113 (1957).
[20] M. Chester, L. C. Yang, and J. B. Stephens, Phys. Rev. Lett. **29**, 211 (1972).
[21] S. M. Lee and J. Krim (to be published).
[22] K. K. Kakati and H. Wilman, J. Phys. D: Appl. Phys. **6**, 1307 (1973).
[23] J. Krim, J. G. Dash, and J. Suzanne, Phys. Rev. Lett. **52**, 640 (1984); G. Palasantzas and J. Krim, Phys. Rev. Lett. **73**, 3564 (1994).
[24] A. Dayo and J. Krim, Int. J. Thermophys. **19**, 827 (1998).
[25] P. M. McGuiggan and J. N. Israelachvili, J. Mater. Res. **5**, 2232 (1990); M. Hirano, K. Shinjo, R. Kaneko, and Y. Murata, Phys. Rev. Lett. **67**, 2642 (1991); **78**, 1448 (1997).